Fermi National Accelerator Laboratory

FERMILAB-Pub-85/119-T
August 1985

Multiple Parton-Parton Interactions in Hadronic Events

TORBJÖRN SJÖSTRAND
Fermi National Accelerator Laboratory
P.O. Box 500, Batavia, IL 60510
and
Department of Theoretical Physics*
University of Lund
Solvegatan 14 A, S-22362 Lund, Sweden

ABSTRACT

Simple models for hadronic events, which involve one parton-parton interaction per event, can not account for a variety of phenomena at collider energies, such as multiplicity distributions or forward-backward correlations. In this paper we develop a simple framework for multiple parton-parton interactions in a single event, and show that this improves agreement with the data. The significance of remaining discrepancies is also discussed.

Oregon Workshop on Super High Energy Physics

*Address after September 15, 1985

variants of the DTU approach, the free parameters in the Pomeron multiplicity distribution are determined by the ratios $\sigma_{elastic}/\sigma_{total}$ and $\sigma_{diffractive}/\sigma_{total}$. Given that these ratios are fairly stable over the explored range of hadronic CM energies $\sqrt{s}$, the Pomeron multiplicity distribution is roughly the same at fixed target energies as at colliders. In a representative model of this kind, the one implemented in ISAJET [5], the resulting variation in mean multiplicity with energy is smaller than is seen in the data. Therefore, fixups have had to be introduced, like making the chain fragamentation function energy-dependent.

One should also note that the predictive power is rather limited for details like how the leading baryon effect arises, how the different chains share the total energy available, how hadrons actually are produced from these chains, what longitudinal and transverse momentum particle spectra one should expect, etc. Even more disturbing, there is no direct link to a perturbative QCD picture for hard parton-parton scatterings.

In different connections it has been pointed out [6-10] that the probability to have several fairly hard parton-parton interactions in one single event is not negligible, particularly not at higher energies. The detailed phenomenology has only been worked out [7,8] for the case of (three or) four high-$p_\perp$ jets resulting from two interactions in the same event. In this paper we want to explore the option of allowing an arbitrary number of parton-parton interactions. Most of these interactions will be fairly soft, but not so soft that the usage of perturbation theory is completely nonsensical ($\Lambda^2 \ll Q^2 \ll s$). Whereas the resulting jets are normally too soft to be observed as such, the concept

of multiple interactions significantly affects our understanding of the ordinary "minimum bias" or "low-$p_\perp$" events. Since this is a first attempt in a new field, we will leave a number of fundamental questions unanswered, and rather try to establish the viability of the "multiple parton-parton interaction" approach as such.

A note on terminology. In the following, we will use the word "scattering" as shorthand for a reasonably hard parton-parton interaction, like $qq \to qq$, $q\bar{q} \to gg$, $qg \to qg$, $gg \to gg$ or $gg \to q\bar{q}$. Indeed, we would prefer to denote our approach "multiple parton-parton scattering", except that this may evoke a picture of one single parton scattering against several partons in the colliding hadron, whereas our main interest will be in interactions between disjoint pairs of partons.

The objective is to give a description for the complete event structure, in as much detail as can be observed experimentally; therefore analytical methods are seldom useful. Instead, all phenomenological investigations have been carried out within the framework of the Lund Monte Carlo. Roughly speaking, the task of setting up the parton configuration resulting from a hard scattering is handled by the PYTHIA routines [11], whereas subsequent fragmentation and decays have been performed by JETSET version 6.1 [12]. One outcome of the present paper is a new version 4.2 of PYTHIA, which obviously is available to interested users.

II. THE NAIVE APPROACH

In order to appreciate the necessity for multiple parton-parton interactions, it may be useful to demonstrate the shortcomings of simpler models. In this section we will introduce these simpler

schemes, which anyhow will be used as building blocks in later sections, and illustate the experimental implications.

In this paper, the Lund model for jet fragmentation [13] will always be used to transform a given parton configuration into experimentally observable particles. This model uses the kinematics of the massless relativistic string with no transverse degrees of freedom, to provide a Lorentz covariant description for the flow of energy and momentum due to a linear confinement potential. In this framework, a quark, diquark, antiquark or antidiquark is considered as an endpoint of the string, whereas a gluon corresponds to a kink on it. The tunneling mechanism is invoked to explain how the string breaks, by the production of new $q\text{-}\bar{q}$ or $qq\text{-}\bar{q}\bar{q}$ pairs, to produce primary hadrons, which then may decay further. This model has a strong support in e^+e^- two- and three-jet phenomenology [14], and has also fared well in comparisons with leptoproduction data [15]. In particular, for hadron-hadron collision studies, we will assume that all parameters of the model have been determined from other data, i.e. we will apply jet universality. For high-$p_\perp$ jets this assumption is probably rather uncontroversial, whereas the validity as to beam jet hadronization is completely unknown.

The simplest possible way to produce a hadronic (inelastic, nondiffractive) event is to have an exchange of a very soft gluon between the two colliding hadrons. Without (initially) affecting the momentum distribution of partons, the "hadrons" become colour octet objects rather than colour singlet ones. If only valence quarks are considered, the colour octet state of a baryon can be decomposed into a colour triplet quark and an antitriplet diquark. In a baryon-baryon collision, one would then obtain a two-string picture [16], with each

string stretched from the quark of one baryon to the diquark of the other, Fig. 1a, whereas a baryon-antibaryon collision would give one string between a quark and an antiquark and another one between a diquark and an antidiquark, Fig. 1b. The two strings are assumed to fragment independently of each other.

It remains to be specified how the two strings should share the available energy. Following [17] one may e.g. choose an ansatz

$$f(x) = \frac{(1-x)^2}{(x^2+c^2)^{\frac{1}{4}}} \tag{1}$$

for the fraction x that the quark takes of the baryon energy, with 1-x going to the diquark. The cutoff $c = 2m_q/\sqrt{s} \approx 0.6$ GeV$/\sqrt{s}$ is not really necessary here, but is included for further reference; the mean value is $\langle x \rangle = 1/7$ for c=0 and larger for nonzero c, i.e. the energy is shared fairly evenly among the three quarks of the original baryon.

In Fig. 2 we compare this model with the UA5 (corrected) data on the charged multiplicity distribution for 540 GeV $p\bar{p}$ interactions [18,19], and we immediately note that the model gives far too narrow a distribution. This is basically the statement that multiplicity distributions in e^+e^- annihilation are much more narrow than in hadron physics (a string corresponds to an e^+e^- two-jet event). The extra element of having two strings that share the energy differently in different events does broaden the distribution, but not enough, even with other f(x) than the one we chose in eq. (1). At this point we should mention that, while well defined single diffractive events have been removed from the data, a not insignificant number of single and

double diffractive events remain. Since such events are not included in the models we study, the discrepancy at small multiplicities need not be that serious; it is the lack of a tail out to large multiplicities that makes the model unacceptable.

Another important observable is the forward-backward multiplicity correlation, Fig. 3. This is defined in the following way. Consider two bins in pseudorapidity, one between $\Delta\eta/2$ and $\Delta\eta/2 + 1$ (forward), the other between $-\Delta\eta/2$ and $-(\Delta\eta/2 + 1)$(backward), i.e. two 1 unit wide bins separated by a central gap of $\Delta\eta$. Call the charged multiplicities in the two bins n_F and n_B, and define the correlation coefficient by

$$b = \frac{\langle n_F n_B \rangle - \langle n_F \rangle^2}{\langle n_F^2 \rangle - \langle n_F \rangle^2} \tag{2}$$

(Where $\langle \ldots \rangle$ means taking average over all events, and where we have explicitly used that $\langle n_F \rangle = \langle n_B \rangle$, $\langle n_F{}^2 \rangle = \langle n_B{}^2 \rangle$). It is this number, b, that is plotted as a function of $\Delta\eta$ in Fig. 3, again compared with UA5 data [19,20]. Apart from a very small short range effect, the model does not predict any forward-backward correlations. This is with the x_1 and x_2 values for the p and $\bar{p}$ sides chosen independently according to eq. (1), but even with $x_1 = x_2$ (event by event) the resulting correlation is only a quarter of the observed one.

A model that only contains partons with low transverse momenta is obviously a simplification. As will be discussed below, the perturbative QCD cross section for a "hard" scattering that gives the two partons transverse momenta of at least 1.6 GeV almost saturates the

inelastic, nondiffractive cross section. Such events will result in different string configurations [11], one example for gg→gg is shown in Fig. 1c. These configurations collapse continuously into the simple two-string picture of Fig. 1a or 1b if the momentum transfer is allowed to go to zero, at least for the dominant one-gluon-exchange graphs. The only place where special care should be taken, at least in principle, is that the function f(x) in eq. (1) should be associated with the $Q^2=0$ limit of valence quark structure functions.

The (aesthetical) urge to have this continuous transition from a high-$p_\perp$ to a low-$p_\perp$ event was actually what made us choose the low-$p_\perp$ model the way we did, rather than using e.g. the one-string Lund low-$p_\perp$ model presented in [21]. The latter model has turned out to be very successful in describing fixed target data [22], and none of the essential deliberations in this paper would have been changed had we used it instead.

The inclusion of hard scatterings actually results in negligible improvements in Figs. 2 and 3. The reason is that most "hard" scatterings still have $p_\perp$ for the scattered partons in the range 1.6-3 GeV, i.e. not enough to make much difference in the event structure.

A hard scattering is, by necessity, associated with the possibility of gluon bremsstrahlung. Our model for initial and final state radiation has been discussed in [23]. If these effects are included, some further improvements are noted in Fig. 2 and 3, but again far from enough.

One effect [24] that does appear at this point, is that the mean charged particle transverse momentum $\langle p_\perp \rangle$ is larger in events with large charged multiplicity n_{ch}. For the low-$p_\perp$ models, $\langle p_\perp \rangle$ is actually

somewhat decreasing with n_{ch} because of secondary decays. This effect is not overcome by introducing hard scatterings, whereas the further introduction of bremstrahlung increases n_{ch} for those events with large $p_\perp$ for the scattered partons.

In conclusion, we note that "one-scattering" models for hadronic events are woefully inadequate. Specifically, the long tail of the data out to large multiplicities is absent in the models. We now proceed to look into the possibility of multiple parton-parton interactions.

III. MULTIPLE PARTON-PARTON INTERACTIONS

The differential cross section for a parton-parton scattering is singular for the momentum transfer $\hat{t}\to 0$ (or $\hat{0}\to 0$), as expressed e.g. in the well-known rule of thumb that the $p_\perp$ spectrum for the partons from a hard scattering should behave roughly like $dp_\perp^2/p_\perp^4$.

In order to better quantify this, define

$$\frac{d\sigma}{dp_\perp^2} = \sum_{ijk} \iiint dx_1 dx_2 d\hat{t} f_i(x_1,Q^2) f_j(x_2,Q^2) \frac{d\hat{\sigma}_{ij}^k}{d\hat{t}} \delta\left(p_\perp^2 - \frac{\hat{t}\hat{0}}{\hat{s}}\right) \qquad (3)$$

where f_i and f_j are the structure functions for finding partons i and j in the two incoming hadrons (for the deliberations in this paper we have used EHLQ set 1 [25]; this is not a crucial assumption) and $d\hat{\sigma}_{ij}^k/d\hat{t}$ is the perturbative QCD cross section for the k:th subprocess for the two partons i,j. The three Mandelstam variables are related by $\hat{s}+\hat{t}+\hat{0} = 0$, with $\hat{s} = x_1 x_2 s$. The definition of Q^2 scale is uncertain and is not crucial, but should roughly be $p_\perp^2$; we have mostly used the combination

$2\hat{s}\hat{t}\hat{u}/(\hat{s}^2+\hat{t}^2+\hat{u}^2)$. The integrated cross section to have a parton-parton scattering above $p_{\perp min}$,

$$\sigma_{hard}(p_{\perp min}) = \int_{p_{\perp min}^2}^{s/4} \frac{d\sigma}{dp_\perp^2} dp_\perp^2 \qquad (4)$$

is $\sigma_{hard}(4\ GeV)\approx 3$ mb, $\sigma_{hard}(3\ GeV)\approx 8$ mb, $\sigma_{hard}(2\ GeV)\approx 22$ mb and $\sigma_{hard}(1\ GeV)\approx 130$ mb at 540 GeV.

The total inelastic, nondiffractive cross section σ_{tot} = 40-50 mb is exceeded for $p_{\perp min}\approx 1.6$ GeV. There is nothing magical about having $\sigma_{hard}(p_{\perp min})>\sigma_{tot}$, however. Sometimes the two colliding hadrons will pass through each other without any single parton being significantly deflected (with "significantly" defined by $p_{\perp min}$). Sometimes there will be one interaction (with $p_\perp > p_{\perp min}$) between two partons, one parton from each hadron. Sometimes there will be two pairwise interactions (each with $p_\perp > p_{\perp min}$), each involving a parton from each of the two hadrons. Sometimes there will be three, or four, or more, interacting parton pairs, with one parton of the pair from each hadron and no pairs sharing any partons (at least to a first approximation). If one wishes, each hadron can be thought of as a "bunch" of partons, with several interactions possible for a single "bunch crossing". The total cross section obviously is the sum of the cross sections for having none, one, two, three, etc., scatterings above $p_{\perp min}$, whereas $\sigma_{hard}(p_{\perp min})$ is the cross section for having one scattering above $p_{\perp min}$, plus twice the cross section for having two such scatterings, plus three times the cross section for three scatterings, etc. In other words, $d\sigma/dp_\perp^2$ counts the inclusive cross sections for having a parton-parton

interaction at the given $p_\perp$ value, i.e. summed over whatever else may be going on in the same event.

Allowing several interactions per event does not solve the problem with $\sigma_{hard}(p_{\perp min})$ diverging for $p_{\perp min} \to 0$. A study of eq. (3) shows that the average $\hat{s}$ of a scattering decreases slower with $p_{\perp min}$ than the number of scatterings increases. One cutoff is then given by the fact that the energy carried off by scattered partons must be removed from further consideration, thus modifying eq. (3). At very high energies, coherence effects [9,26] will also reduce the probability for several interactions to take place close to each other. Neither of these two effects is enough to provide a sensible cutoff at present energies, however.

The more mundane explanation is that, as the transverse momentum of an exchanged gluon is made very small, the gluon transverse size will increase as dictated by the Heisenberg uncertainty relation. Eventually the gluon will no longer be able to resolve the individual colour charges inside a hadron, and effectively no longer couple to the colliding hadrons. In other words, the perturbative matrix elements $d\hat{\sigma}_{ij}^{k}/d\hat{t}$ must have some kind of effective cutoff at the hadronic mass scale. Since the details of this cutoff are unknown, many one-parameter shapes could have been used. For the sake of simplicity and clarity, we have chosen a sharp cutoff at some given $p_{\perp min}$, retaining $d\hat{\sigma}_{ij}^{k}/d\hat{t}$ unchanged above $p_{\perp min}$. By the argument above, one would expect this $p_{\perp min}$ cutoff to be independent of the total energy $\sqrt{s}$ of the collision.

In an event with several scatterings, it is convenient to impose an ordering. The logical choice is to arrange the scatterings in falling sequence of $x_\perp$, i.e. roughly in falling sequence of Q^2. The "first"

scattering is thus the hardest one, with the "subsequent" ("second", "third", etc.) successively softer. It is important to remember that this terminology is in no way related to any picture in physical time; we do not know anything about the latter. In principle, all the scatterings that occur in an event must be correlated somehow, naively by momentum and flavour conservation for the partons from each incoming hadron, less naively by various quantum mechanical effects. When averaged over all configurations of soft partons, however, we should effectively obtain the standard QCD phenomenology for a hard scattering, e.g. in terms of structure functions. Correlation effects, known or estimated, can be introduced in the choice of subsequent scatterings, given that the "preceding" (harder) ones are already known.

With a total number (actually cross section, but choose units so that the luminosity L=1) of hard scatterings $\sigma_{hard}(p_{\perp min})$ to be distributed among the number σ_{tot} events, the average number of scatterings per event is just the ratio $\sigma_{hard}(p_{\perp min})/\sigma_{tot}$. As a starting point, we will assume that the parton-parton interactions in a given hadron-hadron collision take place completely independently of each other. The number of scatterings is then distributed according to a Poissonian with mean $\sigma_{hard}(p_{\perp min})/\sigma_{tot}$. For Monte Carlo generation of these scatterings it is useful to define

$$p(x_\perp) = \frac{1}{\sigma_{tot}} \frac{d\sigma}{dx_\perp} \tag{5}$$

with $x_\perp = 2p_\perp/\sqrt{s}$ and $d\sigma/dx_\perp$ obtained by analogy with eq. (3). Then $p(x_\perp)$ is simply the probability to have a parton-parton scattering at $x_\perp$, given that two hadrons collide.

The probability that the hardest scattering, i.e. the one with highest $x_\perp$, is at $x_{\perp 1}$ is then given by

$$p(x_{\perp 1}) \exp\left(-\int_{x_{\perp 1}}^{1} p(x'_\perp)dx'_\perp\right) \tag{6}$$

i.e. the naive probability to have a scattering at $x_{\perp 1}$ multiplied by the probability that there was no scattering with $x_\perp$ larger than $x_{\perp 1}$. Correspondingly, the probability to have the second hardest scattering at $x_{\perp 2}$ is given by

$$\int_{x_{\perp 2}}^{1} dx_{\perp 1} \exp\left(-\int_{x_{\perp 1}}^{1} p(x'_\perp)dx'_\perp\right) p(x_{\perp 1}) \exp\left(-\int_{x_{\perp 2}}^{x_{\perp 1}} p(x'_\perp)dx'_\perp\right) p(x_{\perp 2}) =$$

$$= p(x_{\perp 2}) \left(\int_{x_{\perp 2}}^{1} p(x'_\perp)dx'_\perp\right) \exp\left(-\int_{x_{\perp 2}}^{1} p(x'_\perp)dx'_\perp\right) \tag{7}$$

i.e. the product of the probabilities to have no scatterings between 1 and $x_{\perp 1}$, to have one at $x_{\perp 1}$, to have none between $x_{\perp 1}$ and $x_{\perp 2}$ and to have one at $x_{\perp 2}$, integrated over all possible $x_{\perp 1}$. In general, for the n:th scattering, the exponentials always sum up to give the integral between $x_{\perp n}$ and 1. The nested integral over scatterings $x_{\perp 1} > x_{\perp 2} > \ldots\ldots > x_{\perp n-1} > x_{\perp n}$ is given by

$$\int_{x_{\perp n}}^{1} dx_{\perp 1} p(x_{\perp 1}) \int_{x_{\perp n}}^{x_{\perp 1}} dx_{\perp 2} p(x_{\perp 2}) \ldots \int_{x_{\perp n}}^{x_{\perp (n-2)}} dx_{\perp (n-1)} p(x_{\perp (n-1)}) =$$

$$= \frac{1}{(n-1)!} \left(\int_{x_{\perp n}}^{1} p(x_{\perp}') dx_{\perp}' \right)^{n-1} \tag{8}$$

so that the probability for a n:th scattering at $x_{\perp n}$ becomes

$$p(x_{\perp n}) \frac{1}{(n-1)!} \left(\int_{x_{\perp n}}^{1} p(x_{\perp}') dx_{\perp}' \right)^{n-1} \exp\left(- \int_{x_{\perp n}}^{1} p(x_{\perp}') dx_{\perp}' \right) \tag{9}$$

The total probability to have a scattering at $x_{\perp}$, irrespectively of it being the first, second or whatever, obviously is

$$\sum_{n=1}^{\infty} p(x_{\perp}) \frac{1}{(n-1)!} \left(\int_{x_{\perp}}^{1} dx_{\perp}' \, p(x_{\perp}') \right)^{n-1} \exp\left(- \int_{x_{\perp}}^{1} dx_{\perp}' p(x_{\perp}') \right) = p(x_{\perp}) \tag{10}$$

The multiple interaction formalism thus retains the correct perturbative QCD expression for the scattering probability at a given $x_{\perp}$.

With the help of the integral

$$P(x_{\perp}) = \int_{x_{\perp}}^{1} p(x_{\perp}') dx_{\perp}' = \frac{1}{\sigma_{tot}} \int_{sx_{\perp}^2/4}^{s/4} \frac{d\sigma}{dp_{\perp}^2} dp_{\perp}^2 \tag{11}$$

(where we assume $P(x_{\perp}) \to \infty$ for $x_{\perp} \to 0$) and its inverse P^{-1} the iterative procedure to generate a chain of scatterings

$x_{\perp 1} > x_{\perp 2} > \ldots\ldots$ is described by

$$x_{\perp i} = P^{-1}\left(P\left(x_{\perp(i-1)}\right) - \ln R_i\right) \tag{12}$$

where the R_i are random numbers evenly distributed between 0 and 1. The iterative chain is started with a fictitious $x_{\perp 0} = 1$ and is terminated when $x_{\perp i}$ is smaller than $x_{\perp min} = 2p_{\perp min}/\sqrt{s}$. Since P and P^{-1} are not known analytically, the standard Monte Carlo procedure is to find a $\tilde{p}(x_\perp) \geq p(x_\perp)$ for all $x_\perp > x_{\perp min}$, with $\tilde{p}$ a particularly simple function, like constant/$x_\perp^3$ (i.e. using the approximate $dp_\perp^2/p_\perp^4$ behaviour noted earlier), which can be analytically integrated and inverted. From the chain thus generated, a given $x_{\perp i}$ is to be retained with probability $p(x_{\perp i})/\tilde{p}(x_{\perp i})$.

In addition, for each $x_\perp$ value chosen, further variables have to be found according to the matrix element. This involves selecting $\tau = x_1 x_2$ and $x_F = x_1 - x_2$ for each incoming parton pair, resolving the twofold ambiguity between $\hat{t}$ and $x_\perp$

$$\hat{t} = -\tfrac{1}{2}\hat{s}\left(1 \pm \sqrt{1 - x_\perp^2/\tau}\right) , \tag{13}$$

choosing flavours for the incoming partons and, where necessary, for the outgoing ones. All this can be handled using standard Monte Carlo techniques, in particular by generalizing $p(x_\perp)$ and $\tilde{p}(x_\perp)$ above to be functions also of τ, x_F etc.

Whereas the ordinary structure functions should be used for the hardest scattering in order to reproduce standard QCD phenomenology, the structure functions to be used for subsequent scatterings must depend on all preceding x values and flavours chosen. We do not know enough about

the hadron wave function to write down such joint probability distributions (some suggestions are found in [27,17,7,8]). To take into account the energy "already" used in harder scatterings, a conservative approach is to evaluate the structure functions, not at x_{kn} for the n:th scattered parton from hadron k, but at

$$x_{kn}' = x_{kn} / \left\{ 1 - \sum_{i=1}^{n-1} x_{ki} \right\} \tag{14}$$

This will be our standard procedure in the following; we have tried a few alternatives without finding any significantly different behaviour in the final physics.

In a fraction $\exp(-P(x_{\perp min}))$ of the events there will be no hard scattering above $x_{\perp min}$ when applying the iterative procedure in eq. (12). In that case we assume that one single soft scattering takes place below $x_{\perp min}$, to give the simple two-string low-$p_\perp$ configuration described in section II.

IV. SOME FIRST RESULTS

The discussion in the previous section does not exhaust the list of model details and uncertainties, but it may be valuable to pause at this point and consider how the model fares when compared with the data.

As we saw, there is one main free parameter in the problem, $p_{\perp min}$. As $p_{\perp min}$ is decreased, the average number of scatterings increases, and so do the fluctuations. Events which contain a large number of scatterings also have large multiplicities. In Fig. 4 it is shown how the multiplicity distribution evolves as $p_{\perp min}$ is decreased from 2.0 to 1.6 to 1.2 GeV. At the same time, the average number of scatterings

increases from 0.56 to 1.01 to 2.11. A fair agreement with the high-multiplicity tail is obtained for $p_{\perp min}$ = 1.6 GeV. The forward-backward correlation is now of significant size, Fig. 5, since the number of scatterings strongly influences the multiplicity in both hemispheres simultaneously. The correlation strength would be further increased by the introduction of diffractive events, which have lower-than-average multiplicity in both hemispheres.

One important constraint is that the mean charged multiplicity should come out in agreement with the data. The experimental number is roughly $\langle n_{ch} \rangle = 29$ [18]; since this is contaminated by diffractive events, we may allow values in the range 30-35 at the present stage of the game. As it is, the simple two-string low-$p_\perp$ model gives $\langle n_{ch} \rangle = 28$ by itself, so there would have been little room for multiple scatterings. In order to avoid this, we had to reject the shape of eq. (1) and instead adopt

$$f(x) = \frac{(1-x)^3}{(x^2+c^2)^{\frac{1}{2}}} \tag{15}$$

which, at 540 GeV, has $\langle x \rangle = 0.044$ rather than the 0.148 of eq. (1). This decreases the low-$p_\perp$ model $\langle n_{ch} \rangle$ to 23. Including multiple interactions, the distributions for $p_{\perp min}$ = 2.0, 1.6 and 1.2 GeV then have $\langle n_{ch} \rangle$ = 29,33 and 42, respectively.

Some further improvements are to be had by making the x distribution even more asymmetrical. An extreme case is provided by the Lund one-string low-$p_\perp$ model [21], which by itself has $\langle n_{ch} \rangle$ = 17. If this model is used for all events that do not contain a hard scattering,

and eq. (15) is used (when needed) for events containing at least one hard scattering, $p_{\perp min} = 1.5$ GeV in many respects gives a fair agreement with the data. Also part of the "missing" low-multiplicity events are now included, and as a result the forward-backward correlation strength is increased to the level of the data. However, the discontinuity in physics between high-$p_\perp$ and low-$p_\perp$ events shows up as an ugly dip in the multiplicity distribution around $\langle n_{ch} \rangle = 25$, so we are forced to reject such a scenario.

In conclusion, from now on we will use $p_{\perp min} = 1.6$ GeV and eq. (15) as our standard scenario for multiple interactions. In particular, we will assume that the $p_{\perp min}$ value is independent of the collision energy $\sqrt{s}$. The $p_{\perp min}$ determination masks a large number of uncertainties in the model, so that e.g. a modification in the handling of structure functions for secondary scatterings, naively changing the average number of scatterings and thus agreement with the multiplicity distribution, could be compensated by a shift in the $p_{\perp min}$ value.

The interpretation of "hot spots" in the UA5 data [28] is a useful illustration to the importance of multiple interactions. The experimental definition of a hot spot is a 0.5 units of pseudorapidity wide region, containing at least $6.7 + 0.1\, n_{ch}$ charged particles, where n_{ch} is the total charged multiplicity of the event. In 6339 events 47 hot spots were found, or 0.0074 per event. Naive low-$p_\perp$ models give roughly a factor 20 too low a rate. Even with the inclusion on one hard scattering above 1.6 GeV and initial and final state radiation, the rate is only a third of the desired one. In a multiple interaction Monte Carlo run, 8801 events produced 65 hot spots, giving exactly the experimental rate. Further, where data showed that events with hot

spots had a average charged multiplicity of 47, and a pseudorapidity plateau height of 7 around the spot, the corresponding numbers for the Monte Carlo events were 48.5 and 6.5, respectively.

V. LIMITATIONS IN THE MODEL

In this section we will discuss some further details of the model, in particular those where the present paper may be considered as a "first pass" attempt, that could be improved on by further work.

One major problem, not discussed so far, is the question of colour flow. In simpleminded independent fragmentation models, like ISAJET, all outgoing partons are assumed to fragment independently of each other, however close they are. Such a scenario is contradicted by e^+e^- data [14]. In the Lund model [13], colour strings are attached to the partons, with one string piece attached to each quark and two to each gluon, corresponding to the larger colour charge of a gluon. In [29,11] it has been discussed how ambiguities arise for parton-parton scatterings in hadron physics. To a first approximation, the standard perturbative QCD cross sections can be subdivided into different pieces, each with a well defined colour flow structure. Unfortunately, the cross sections also contain pieces, down in relative magnitude by $1/N_C^2$ with $N_C = 3$ the number of colours, which correspond to interference terms between different possible string drawings. A working scheme can be obtained by neglecting those terms, or by distributing them among the well defined pieces in some fashion [11].

The different colour flow configurations directly link the hard scattering partons to the hadron beam remnants, by virtue of each remnant carrying the opposite colour charge to whatever parton from it

partook in the hard scattering. For the case of a gluon being scattered out of a baryon, the baryon remnant could be subdivided into a quark and a diquark, giving the endpoints for the colour flow. In a multiple interaction framework a number of quarks, antiquarks and gluons are scattered out of the incoming hadron, and the situation is considerably more complex. The (non-Abelian) colour charges of the scattered partons can add up in different fashions, sometimes giving a large net charge to the hadron remnant. We do not know how to calculate the relative probability for different net colour charges, nor how to handle beam remnants with large charges. Therefore we have tried two simple schemes, and feel somewhat encouraged by the fact that these give almost the same results.

As a first simplification, after the first (hardest) scattering has been found, it is assumed that all subsequent scatterings are of the type gg→gg. This way we do not have to consider e.g. hadron remnants where all the valence quarks have been scattered. The approximation is not a completely nonsensical one, in that the gg→gg subprocess indeed is the largest piece in the scattering cross section for small $p_\perp$ values, where most of the scatterings take place. Since qg→qg is not negligible, and since a q has a somewhat larger average x value, we have also used the full matrix element in the choice of x_1 and x_2 values for the two incoming partons, although both in the end were then assumed to be gluons. Differences between using the full matrix element or only the gg→gg one can be pushed into the choice of $p_{\perp min}$ value; $p_{\perp min} = 1.6$ GeV was determined using the full cross section.

A first, simple scheme is to assume that each gg pair forms a colour singlet for all the subsequent (i.e. non-first) gg→gg scatterings. Then each such scattering just gives rise to a closed gluon loop (a double string) stretched between the two scattered gluons, Fig. 6a. Although differing in the details, such a scenario is actually reminiscent of the DTU approach, where each real Pomeron exhcange gives rise to a "double string" with vanishing net flavour content [1-5]. The colour structure of the beam remnants is completely determined by the first scattering, which is handled in the standard fashion [11]. (Because of its ruggedness it is actually this, and not the following scenario, that is implemented in the publicly available PYTHIA version 4.2).

A more complex scheme is to define the colour flow of each scattering using the customary relative probabilities, but to require that the magnitude of the colour charge given to the beam remnants by the first scattering stays fixed. For each of the subsequent gg→gg scatterings, one triplet or antitriplet colour charge of each beam remnant gets "rerouted" and another one is attached, Fig. 6b. The physics behind such an assumption could be a desire on behalf of nature to avoid a buildup of a large colour charge in a beam remnant, so that the colour charges of removed partons are correlated. Alternatively, one could really imagine a beam remnant with a large net colour charge, but with gluons carrying most of this. In the limit of vanishing momentum the only effect of such a gluon would then be to "reroute" the colour charge in just the desired way. In this case, the model should be extended to include a distribution function in momentum fraction x for these beam remnant gluons. In the former case, when the existence

of such gluons is not invoked, the problem arises that occasionally a closed gluon loop may turn out to consist of just one gluon, Fig. 6c. The colour amplitude for such a graph as a whole must obviously be vanishing, but in our simplified treatment we only know the colour amplitude expressions for the subgraphs, which each by itself is nonvanishing. Therefore some extra rules have to be introduced, on how to modify the colour flow in case of failure. It is exactly this course we have implemented as the second sceme.

When comparing the two schemes, Figs. 6a and 6b, again differences are marginal, at least at present energies. On the average, the latter gives a slightly larger multiplicity, if the same $p_{\perp min}$ is used. This is because the matrix element for gg→gg is peaked for the gg invariant mass being close to the lower cutoff, $2p_{\perp min}$, but with different scatterings centered at slightly different rapidities ($y = \frac{1}{2}\ln x_1/x_2$ for two incoming partons at x_1 and x_2). Then the average gg→gg subsystem mass is somewhat smaller than the average mass of two gluons taken from two different scatterings centered at different rapidities.

The inclusion of initial and final state radiation for each scattering would lead to further complications with string drawing issues. In the present paper we have therefore only allowed such radiation related to the first scattering. Since subsequent scatterings usually are at low $p_\perp$ values, where radiation effects are small, this is probably not a bad first approximation.

A more serious problem is the simpleminded space-time picture used for hadron collisions, specifically that we have considered all nondiffractive, inelastic events to be equivalent. This is true e.g. for e^+e^- annihilation, but in hadron collisions there is an impact

parameter which varies from event to event. A small impact parameter, i.e. a central collision, corresponds to a sizeable overlap of the hadronic matter of the two colliding partons, and the average number of parton-parton scatterings is high. Correspondingly, a large impact parameter, i.e. a peripheral collision, is associated with a small number of parton-parton scatterings. When integrated over all impact parameters, the standard perturbative QCD cross sections must obviously be recovered. At present collider energies, where the mean number of scatterings per event is of order unity, this underestimation of event-by-event fluctuations probably is not very important, either for the overall multiplicity distribution or the forward-backward correlation. At higher energies (and hence higher mean number of scatterings) the impact parameter degree of freedom is likely to play an important rôle.

In order to quantify this effect better, one would have to have a model for the spatial distribution of energy inside a (fast) hadron, and study the hadron-hadron energy overlap pattern. This is an interesting field for further study. An indication of the size of the effect can be obtained by comparing the jet energy profile obtained in our model with the measured UA1 one [30]. The requirement of a hard jet in the event implies that these events very likely have small impact parameters, and therefore should contain an above average number of extra scatterings. The result presented in [23], with initial and final state showers included, but without multiple interactions, is given in Fig. 7, together with the new results obtained with multiple interactions. As can be seen, the wings of the distribution, i.e. the "pedestal", are still too low. If the probability for multiple interactions is

increased by a factor of four for these events, one obtains fair agreement with the data. Of course, neither data nor model can be trusted enough to give more than a rough estimate, a factor three or five rather than four is by no means excluded.

Technically, the change in the program is done by using a $\sigma_{tot} = 12$ mb, rather than 47mb, in eq. (5). Of course in that case σ_{tot} should no longer be thought of as a cross section, but rather as the effective size of the hadronic matter. Thus the result, at first sight maybe counterintuitive, that a smaller σ_{tot} gives a larger average number of scatterings. A suitable average over the individual σ_{tot} values for events must of course give back the conventional number.

It should be noted that the need for a higher multiple interaction probability in events with a hard jet is related to our use of string fragmentation, and the same conclusion is not reached when using independent fragmentation. (This was first noted running the Lund Monte Carlo in its independent fragmentation mode, but has recently been confirmed by ISAJET results [31]). This is because initial state radiation, associated with the presence of a hard scattering, results in a number of partons traveling more or less parallel to the beam remnants. These partons produce a sizeable number of hadrons when allowed to fragment independently of each other (in the CM frame of the two colliding hadrons). In particular, since the results for independent fragmentation are sensitive to the choice of parton shower cutoffs, a suitable tuning of the initial state radiation cutoff can produce the desired "pedestal" height. It would be very useful to find out how to distinguish these two scenarios from each other experimentally. An obvious place to look is in electron-proton

collisions at HERA, where multiple scattering effects are virtually absent.

Finally, two further complications. In addition to having new pairs of partons for each subsequent scattering, occasionally one single parton from one of the incoming hadrons may successively scatter against two different partons from the other hadron [7]. Also, the Altarelli-Parisi Q^2 evolution of the structure functions implies that two partons from the same hadron, which at high Q^2 appear to be seperate and each may scatter against partons in the colliding hadron, in fact come from the same "initial" low-Q^2 parton. Our limited understanding of the hadron wave function is a limiting factor to the modeling of either of these effects.

VI. ENERGY DEPENDENCE

Now, having commented on limitations, uncertainties and faults, we will take the model at face value and present some predictions, specifically with respect to energy dependence.

In Table I, some results at different energies are summarized, all for the case of $p\bar{p}$ collisions (results for pp would be rather similar). The σ_{tot} values, necessary as input, are rough estimates. The increase with energy in the average number of scatterings is slowed down by the increase in σ_{tot} ; the latter effect is likely dominated by an increase in the number of peripheral (large impact parameter) collisions.

The increase in the average number of parton-parton scatterings per event is our main point of disagreement with the DTU approach, at least as implemented in ISAJET at present [5], where an essentially

energy-independent Pomeron multiplicity distribution is used. As a result, whereas the present program and ISAJET agree on the average charged multiplicity at present collider energies, by virtue of both programs having been tuned to agree with existing data, the programs disagree significantly at SSC energies (40 TeV): our prediction of 134 is a factor of two higher than the ISAJET number, 68 [32]. The number 134 would have been 81 without multiple interactions and 43 if no high-$p_\perp$ scatterings at all were included.

For comparisons with recent collider runs, we again emphasize the lack of diffractive events in the model. Using the 540 GeV data [18] to fix a rescaling factor 29/32, the predicted number at 200 GeV is 21 and at 900 GeV 35. This should be compared with the preliminary UA5 numbers [32], 22.1±0.7 and 34.6±0.7, respectively.

The mean transverse momentum is given for charged particles with pseudorapidity $|\eta|<2$, as might be measurable in a central detector. Results for the full pseudorapidity range are roughly a factor 0.9 lower. The increase in mean transverse momentum is obviously due to the increasing phase space for hard parton-parton scatterings.

The KNO [34] plots of scaled multiplicity distributions have been very much appreciated in recent years. In particular, great emphasis has been placed on understanding the pattern of KNO scalebreaking, e.g. using fits to negative binomial distributions [35]. Our results for the KNO distribution at 20, 63 and 540 GeV are compared with the experimental data in Fig. 8 [18]. The lack of diffractive events leads to a too high mean value $\langle n \rangle$. Therefore the theoretical curves are somewhat compressed in the $n/\langle n \rangle$ variable, even when the n distributions by themselves agree fairly well with the data, cf. Fig. 4. The pattern

of scalebreaking is the same in model and data, however.

It should be emphasized that our "explanation" for the KNO distributions bears very little resemblance to much of the extensive theoretical literature on the subject, where one simple underlying principle is sought (for a few examples see [36]). In our approach, the approximate KNO scaling appears more or less by chance, and receives contributions from (at least) five sources. The basis is obviously formed by the ordinary fluctuations appearing in the fragmentation of a single string. Even in the simple low-$p_\perp$ model, however, additional fluctuations arise because the energy has to be shared between the two strings. When including a not insignificant fraction of hard parton-parton scatterings at higher energies, there are fluctuations in the kinematical variables for each scattering, and also in the associated initial and final state radiation pattern. Further, the fluctuations in the number of scatterings (each having the kinematical variable fluctuations noted above) is added. Finally, not yet studies in detail, we expect the basic probability for multiple scatterings to vary from event to event depending on the impact parameter of the hadron-hadron collision. Actually, in the lack of the latter component, the present multiple interaction framework does not predict a significant additional KNO scalebreaking between 540 and 1600 GeV.

To conclude this section, in Fig. 9 we show how the charged multiplicity is built up for a truly hard SSC scattering, with a $p_\perp$ for each of the two scattered partons of at least 500 GeV. In a "bare bones" picture, without any initial or final state radiation or any multiple interaction contribution, the expected mean charged multiplicity would have been 72. Including final state radiation

increases this to 115; with initial state radiation as well we reach 210. The naive inclusion of multiple interactions, with σ_{tot} = 100 mb, increases the figure to 265; assuming that the multiple interaction probability actually should be a factor four higher for these central collisions (i.e. an effective σ_{tot} = 25 mb) gives 433. In the latter case, there is an average of 14 scatterings per event, so destructive interference between different interactions [9,26] might here be nonnegigible and limit the numbers somewhat. As a best present estimate, we therefore assume roughly 350-400 charged particles per event, up by about a factor of 3 compared to the minimum bias background.

The likely appearance of very high multiplicities at SSC energies has been pointed out before this by Field [37]; a charged multiplicity of 345 (and a total hadronic one of 598) is predicted for the same kind of events as above. This is without any multiple scattering formalism, however, and could be compared with our number 210. The discrepancy of a factor of 1.5 is probably mainly due to our usage of different fragmentation schemes (cf. our discussion about the jet energy profile in section V). Were we to use independent fragmentation rather than string fragmentation, we obtain 340 for the g=q option and 460 for the $g \rightarrow g\bar{g}$ one [12], without invoking multiple interactions. Additionally, for independent fragmentation, the figures are sensitive to the choice of parton shower cutoffs (normally we use Q^2_{cut} = 4 GeV^2 both for timelike and spacelike showers).

VII. CONCLUDING REMARKS

In this paper we have developed and explored a simple formalism for multiple parton-parton interactions within a single hadron-hadron collision. Throughout the paper, we have tried to give an honest assessment of the weak points in the present approach. Whereas that list indeed may seem discouragingly long, the compound uncertainty may still be at a level where it makes sense to use models of this kind. In particular, several of the problems are hidden behind the necessity to determine the cutoff parameter $p_{\perp min}$ from experimental data anyhow.

One may worry about details, but it should always be remembered that the presence of multiple interactions is an inevitable consequence of our standard perturbative QCD picture for hadronic interactions. The question is only at what level these phenomena appear. Here we have argued that the shape of the multiplicity distribution and the forward-backward multiplicity correlation, each by itself points to the need for a nonnegligible multiple interaction contribution at collider energies.

We have in this paper tried to clear away the underbrush, and isolate the areas where further progress is needed. This includes obtaining a better understanding how the perturbative matrix elements are cut off at the hadronic mass scale, how the shape of the hadronic wave function builds up the impact parameter dependence of the multiple interaction probability, how the colour flow between the scattered partons and the beam remnants is arranged, and how the total, diffractive and elastic cross sections are related. Many of these questions have already been discussed within the framework of Dual

Topological Unitarization, but we disagree with a few of the assumptions normally made in this approach.

One advantage with the present approach, is that the model is publicly available in the form of a Monte Carlo program, that can be used by experimentalists to compare directly with data. It is sobering to realize that, if major disagreements between model and data are found, it very likely signals that nature has seen fit to make the physics of hadron-hadron collisions even more complicated than suggested by the present paper.

ACKNOWLEDGEMENTS

The major part of this work was carried out while participating in the Oregon Workshop on Super High Energy Physics at the Institute for Theoretical Science, University of Oregon, Eugene, Oregon. We gratefully acknowledge the stimulating and enjoyable atmosphere provided by the organizers, N. Deshpande, R. Hwa and D. Soper, as well as the co-participants, in particular T. Gottschalk and F. Paige. The work was begun and finished while visiting Fermilab, supported by Swedish Natural Science Research Council post-doc grant F-PD 1559-101. The hospitality of the Fermilab theory group is gratefully acknowledged.

REFERENCES

1. V.A. Abramovski, O.V. Kancheli, V.N. Gribov, in Proc. of XVI International Conference on High Energy Physics, Eds. J.D. Jackson, A. Roberts, R. Donalson, Vol. 1, p. 389
2. A. Capella, J. Tran Thanh Van, Phys. Lett. 114B (1982) 450, Z. Physik C18 (1983) 85, Z. Physik C23 (1984) 165
3. P. Aurenche, F.W. Bopp, Phys. Lett. 114B (1982) 363
   P. Aurenche, F.W. Bopp, J. Ranft, Z. Physik C23 (1984) 67, Z. Physik C26 (1984) 279, Phys. Lett. 147B (1984) 212
4. A.B. Kaidalov, Phys. Lett. 116B (1982) 459
   A.B. Kaidalov, K.A. Ter Martirosyan, Phys. Lett. 117B (1982) 247
5. F.E. Paige, S.D. Protopopescu, in Proc. of 1982 Snowmass Summer Study on Elementary Particle Physics and Future Facilities, Eds. R. Donaldson, R. Gustafson, F. Paige, p. 471
6. P.V. Landshoff, J.C. Polkinghorne, Phys. Rev. D18 (1978) 3344
   C. Goebel, D.M. Scott, F. Halzen, Phys. Rev. D22 (1980) 2789
7. N. Paver, D. Treleani, Nuovo Cimento 70A (1982) 215, Nuovo Cimento 73A (1983) 392, Phys. Lett. 146B (1984) 252, Z. Physik C28 (1985) 187
8. B. Humpert, Phys. Lett. 131B (1983) 461
   B. Humpert, R. Odorico, Phys. Lett. 154B (1985) 211
9. L.V. Gribov, E.M. Levin, M.G. Ryskin, Physics Reports 100 (1983) 1
10. J.C. Collins, in Proc. of 1984 Snowmass SSC Summer Study, Eds. R. Donaldson, J.G. Morfin, p. 251,
    L. Durand, ibid., p. 258

11. H. -U. Bengtsson, Computer Phys. Comm. 31 (1984) 323
H. -U. Bengtsson, G. Ingelman, Computer Phys. Comm. 34 (1985) 251
12. T. Sjöstrand, Computer Phys. Comm. 27 (1982) 243
13. B. Andersson, G. Gustafson, G. Ingelman, T. Sjöstrand, Phys. Rep. 97 (1983) 33,
T. Sjöstrand, Nucl. Phys. B248 (1984) 469
14. JADE Collaboration, W. Bartel et al., Phys. Lett. 101B (1981) 129, Z. Physik C21 (1983) 37
TPC Collaboration, H. Aihara et al., Z. Physik C28 (1985) 31
15. EMC Collaboration, J.J. Aubert et al., Phys. Lett. 100B (1981) 433
EMC Collaboration, M. Arneodo et al., Phys. Lett. 149B (1984) 415
16. A. Capella, U. Sukhatme, C.I. Tan, J. Tran Thanh Van, Phys. Lett. 81B (1979) 68
17. A. Capella, J. Tran Thanh Van, Z. Physik C10 (1981) 249
18. UA5 Collaboration, G.J. Alner et al., Phys. Lett. 138B (1984) 304
19. J. Gaudaen, Ph. D. thesis, Universiteit Antwerpen (1984)
20. UA5 Collaboration, K. Alpgard et al., Phys. Lett. 123B (1983) 361
21. B. Andersson, G. Gustafson, I. Holgersson, O. Mansson, Nucl. Phys. B178 (1981) 242
22. E.A. De Wolf, Z. Physik C22 (1984) 87
23. T. Sjöstrand, Phys. Lett. 157B (1985) 321
24. UA1 Collaboration, G. Arnison et al., Phys. Lett. 118B (1982) 167
25. E. Eichten, I. Hinchliffe, K. Lane, C. Quigg, Rev. Mod. Phys. 56 (1984) 579
26. A.H. Mueller, in preparation

27. J.Kuti, V.F.Weisskopf, Phys. Rev. D4 (1971) 3418
H.R. Gerhold, Nuovo Cimento 59A (1980) 373

28. J.G. Rushbrooke, in Proc. of $p\bar{p}$ Options for the Supercollider, Eds. J.E. Pilcher, A.R. White, p. 176

29. G. Gustafson, Z. Physik C15 (1982) 155

30. UA1 Collaboration, G. Arnison et al., Phys. Lett. 132B (1983) 214

31. F.E. Paige, S.D. Protopopescu, private communication
F.E. Paige, to be published in the proceedings of the International Symposium on Multiparticle Dynamics, Kiryat Anavim, Israel, June 1985

32. J. Lach, private communication

33. J.G. Rushbrooke (UA5 Collaboration), CERN-EP/85-124

34. Z. Koba, H.B. Nielsen, P. Olesen, Nucl. Phys. B40 (1972) 317

35. UA5 Collaboration, G.J. Alner et al., CERN-EP/85-62

36. P. Carruthers, C.C. Shih, Phys. Lett. 127B (1983) 242
C.S. Lam, M.A. Walton, Phys. Lett. 140B (1984) 246
B. Durand, S.D. Ellis, in Proc. of 1984 Snowmass SSC Summer Study, Eds. R. Donaldson, J.G. Morfin, p. 251
G. Pancheri, Y. Srivastava, M. Pallotta, Phys. Lett. 151B (1985) 453

37. R.D. Field, in Proc. of 1984 Snowmass SSC Summer Study, Eds. R. Donaldson, J.G. Morfin, p. 713,
J. Huston, ibid., p. 212

TABLE I

Results from Monte Carlo runs for $p\bar{p}$ collisions at various energies $\sqrt{s}$, taking the nondiffractive, inelastic cross section to be σ_{tot}. $\langle n_{scat} \rangle$ is the average number of parton-parton scatterings, $\langle n_{ch} \rangle$ the average charged multiplicity and $\langle p_\perp \rangle$ the mean transverse momentum for charged particles with pseudorapidity $-2<\eta<2$.

$\sqrt{s}$ (GeV)	σ_{tot} (mb)	$\langle n_{scat} \rangle$	$\langle n_{ch} \rangle$	$\langle p_\perp \rangle$ (GeV/c)
20	29	0.016	8.8	0.36
63	29	0.17	14	0.38
200	35	0.56	23	0.41
540	47	0.90	32	0.43
900	51	1.14	39	0.44
1600	57	1.48	48	0.45
5000	70	2.28	72	0.48
15000	85	2.95	100	0.53
40000	100	3.77	134	0.56

FIGURE CAPTIONS

Fig. 1. Schematic view of colour string drawing in hadron-hadron collisions. Full lines indicate strings, dashed outline outgoing hadrons, with a dot for each valence quark (antiquark) and an extra ellipse marking a diquark (antidiquark).

a) Baryon-baryon collision

b) Baryon-antibaryon collision

c) Baryon-antibaryon collision containing a hard gluon-gluon scattering.

Fig. 2. Charged multiplicity distribution at 540 GeV, UA5 results [18] vs. simple models: dashed low-$p_\perp$ only, full including hard scatterings, dash-dotted also including initial and final state radiation.

Fig. 3. Forward-backward multiplicity correlation at 540 GeV, UA5 results [19] vs. simple models; latter with notation as in Fig. 2.

Fig. 4. Charged multiplicty distribution at 540 GeV, UA5 results [18] vs. multiple interaction model: dashed $p_{\perp min}$ = 2.0 GeV, full $p_{\perp min}$ = 1.6 GeV, dash-dotted $p_{\perp min}$ =1.2 GeV.

Fig. 5. Forward-backward multiplicity correlation at 540 GeV, UA5 results [19] vs. multiple interaction model; latter with notation as in Fig. 4.

Fig. 6. Very schematic view of colour string drawing for multiple interaction events, drawn for the case of two gg→gg scatterings. For notation see Fig. 1; additionally dash-dotted lines from scattered gluons indicate how strings would have

been drawn to the beam remnants if each interaction had been considered on its own, whereas vertical dash-dotted lines inside hadron remnants indicate how the colour gets rerouted.

a) Hardest scattering (uppermost) connected to beam remnants, subsequent scatterings give double string between outgoing gluons.

b) Colours are originally connected to the beam remnants for each scattering, but are then rerouted to give double strings between outgoing gluons coming from different scatterings.

c) Example how the colour flow can conspire to give a gluon (second from top) that naively does not have any partners.

Fig. 7. Jet energy profile, UA1 data [30] vs. model results: dashed without multiple scatterings [23], full with multiple scatterings, dash-dotted with multiple scattering rate increased by a factor four.

Fig. 8. KNO distributions, data (compiled in [18]) vs. model results: dashed $\sqrt{s}$ = 20 GeV, full 63 GeV, dash-dotted 540 GeV.

Fig. 9. Charged multiplicity distribution for hard scattering events, $p_{\perp hard} > 500$ GeV, at 40 TeV: long dashes simple hard scattering with beam jets, dotted including final state radiation, full also including initial state radiation, dash-dotted adding on normal amount of multiple scattering, short dashes with multiple scattering rate increased by a factor four.

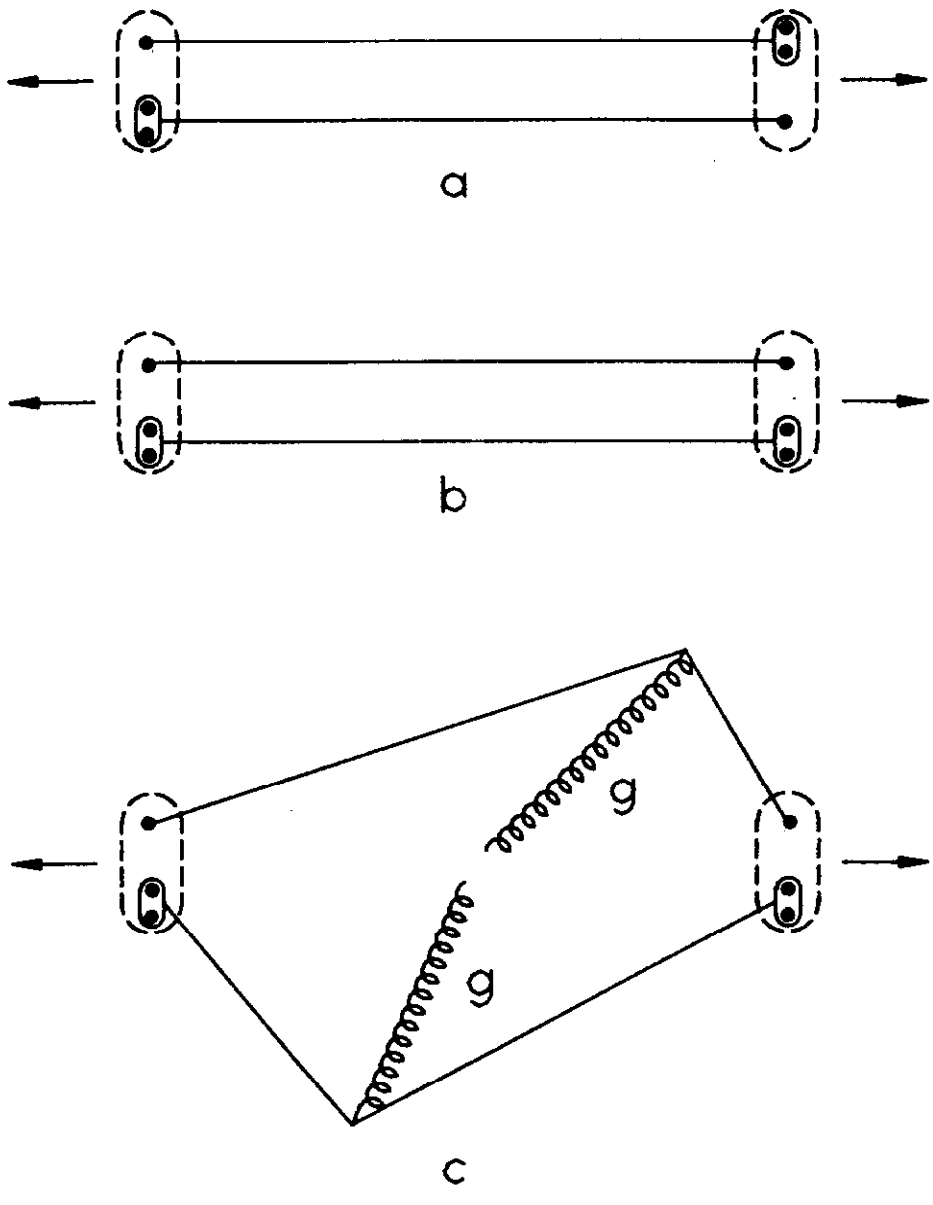

FIG. 1

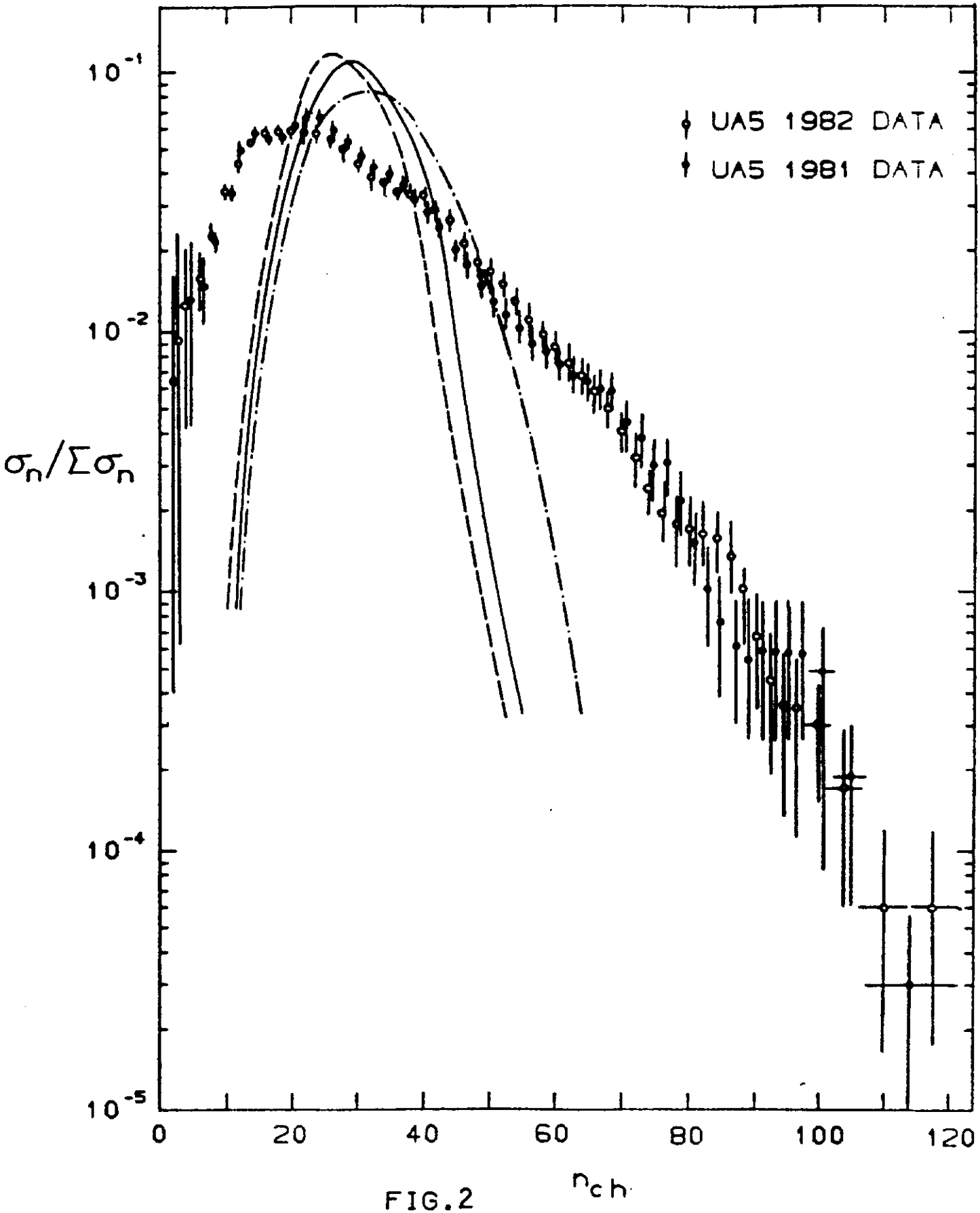
UA5 1982 DATA
UA5 1981 DATA
10^{-1}
10^{-2}
10^{-3}
10^{-4}
10^{-5}
$\sigma_n/\Sigma\sigma_n$
0
20
40
60
80
100
120
n_{ch}

FIG.2

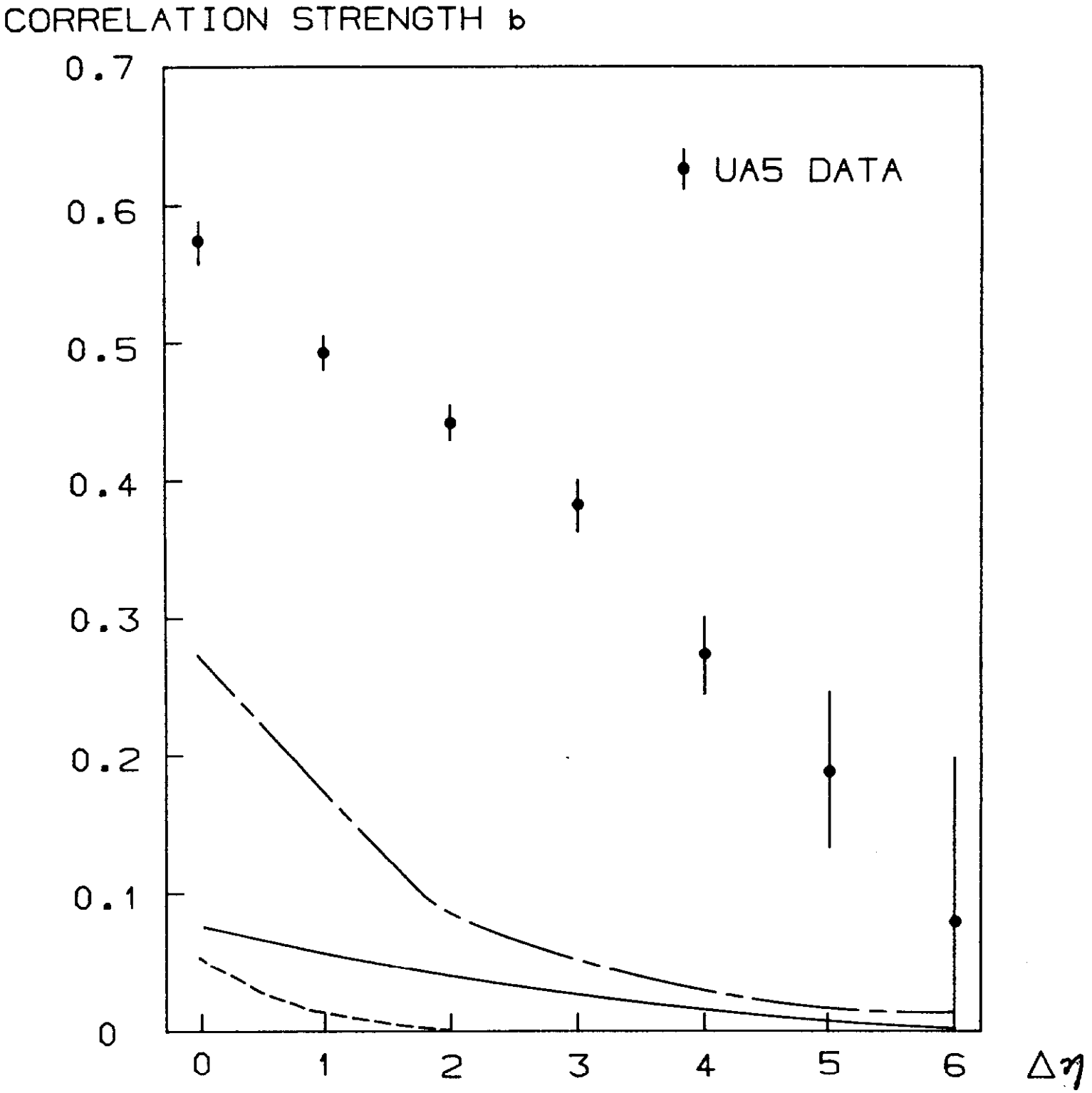
CORRELATION STRENGTH b
0.7
0.6
0.5
0.4
0.3
0.2
0.1
0
UA5 DATA
0
1
2
3
4
5
6
Δη

FIG. 3

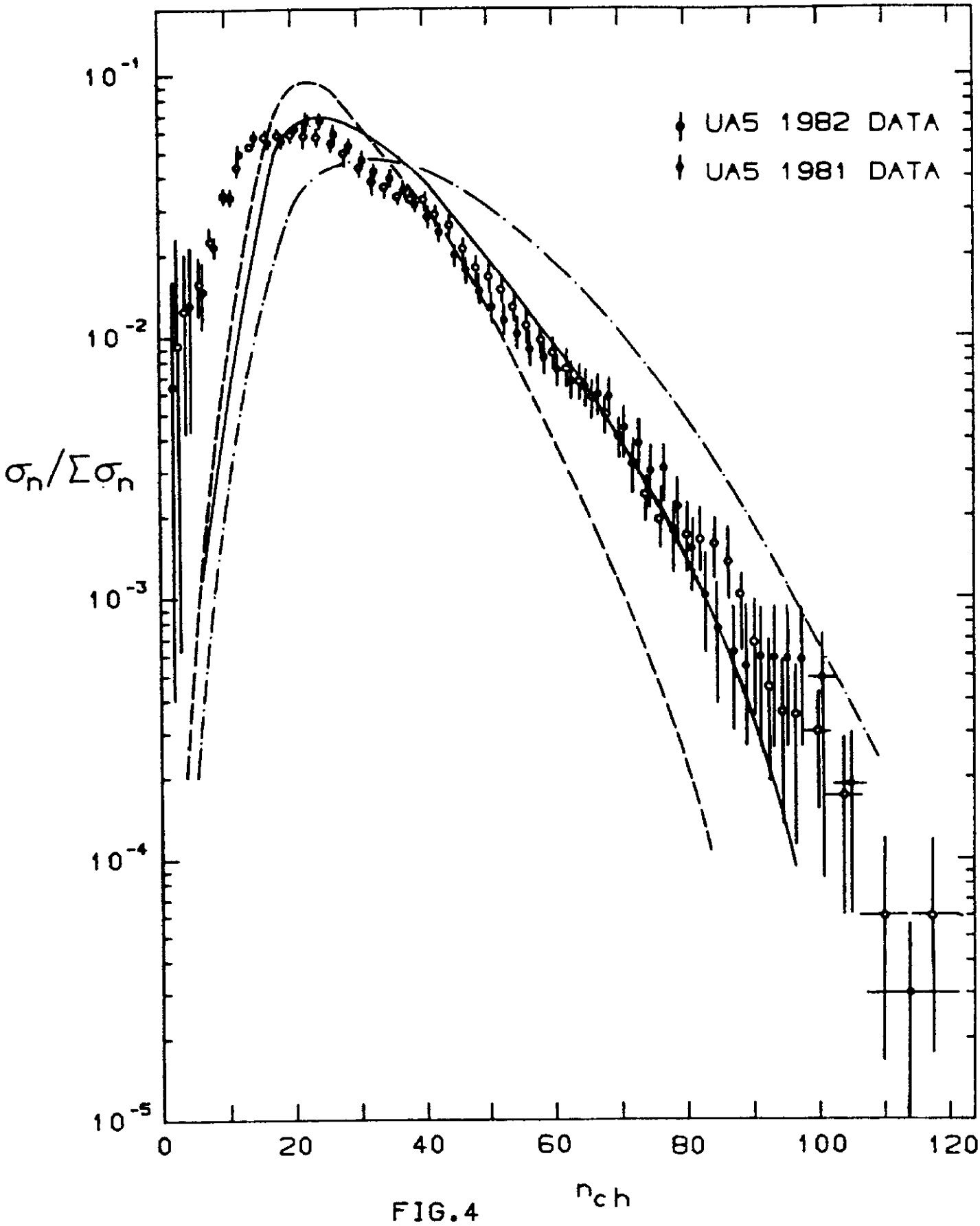
UA5 1982 DATA
UA5 1981 DATA
10^{-1}
10^{-2}
10^{-3}
10^{-4}
10^{-5}
$\sigma_n/\Sigma\sigma_n$
0
20
40
60
80
100
120
n_{ch}

FIG.4

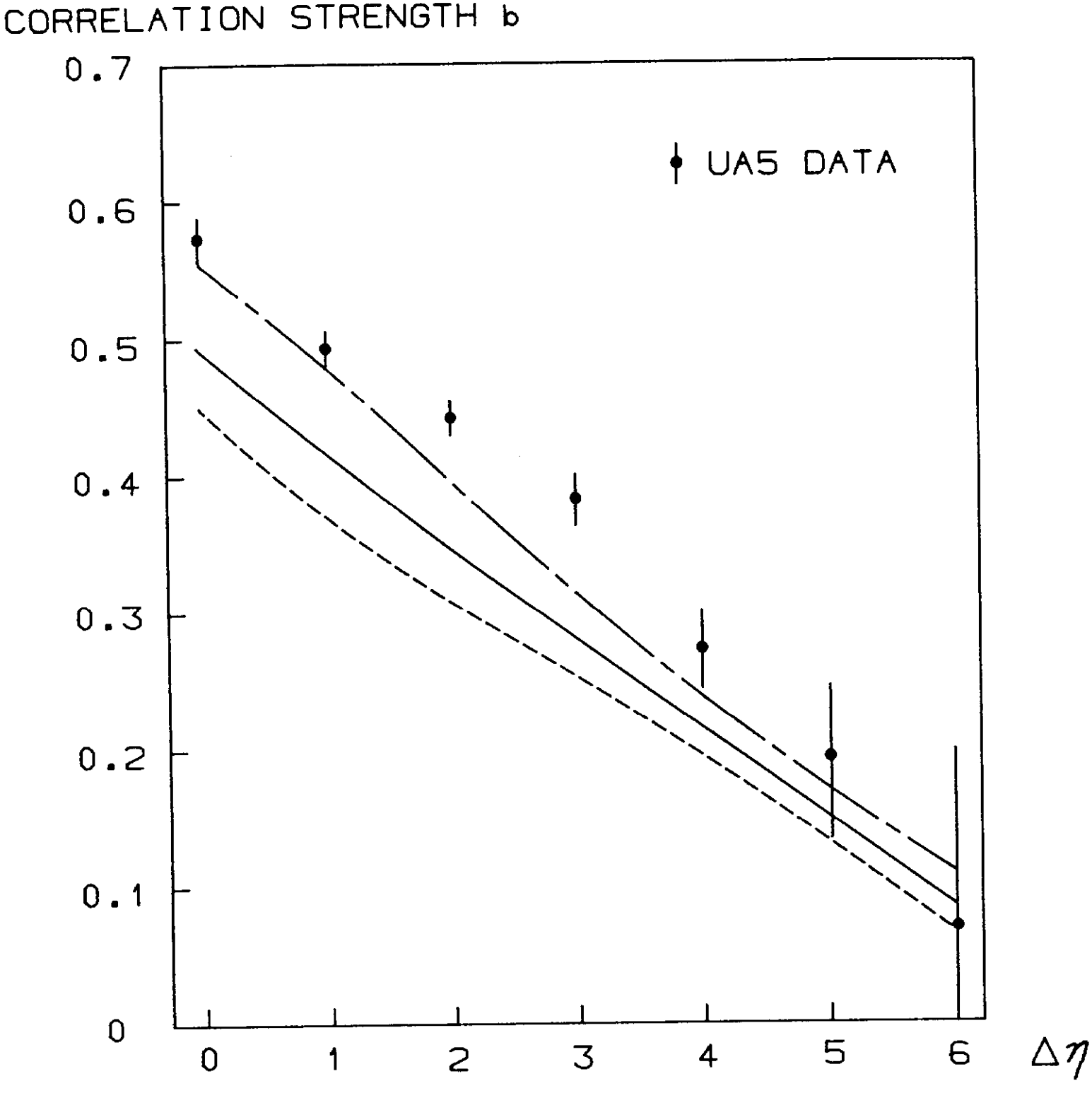
CORRELATION STRENGTH b
0.7
0.6
0.5
0.4
0.3
0.2
0.1
0
UA5 DATA
0
1
2
3
4
5
6
Δη

FIG. 5

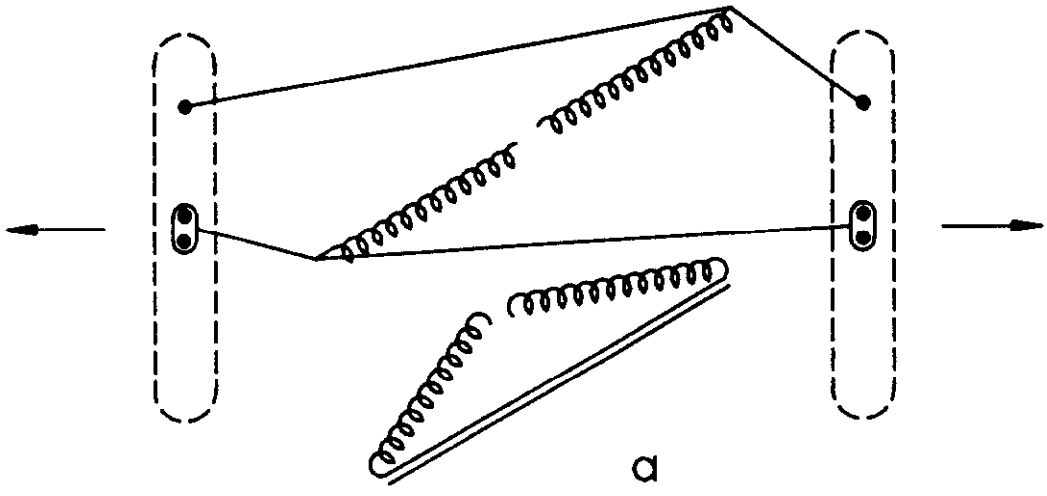

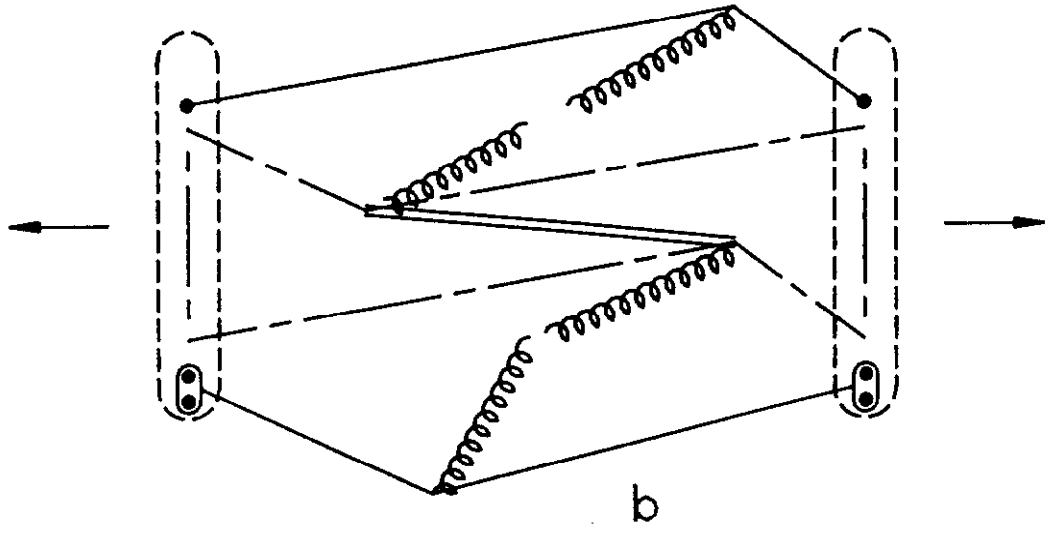

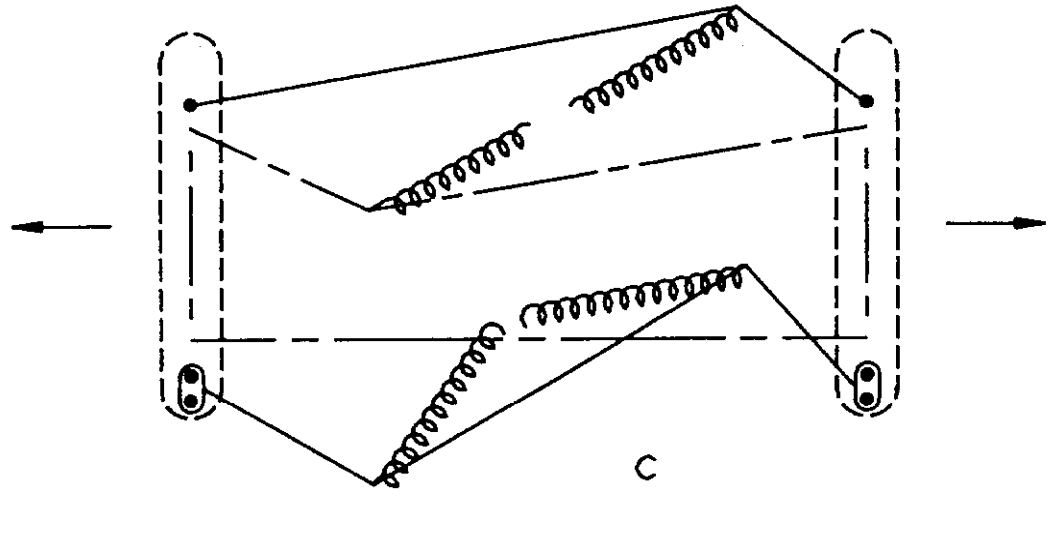

FIG. 6

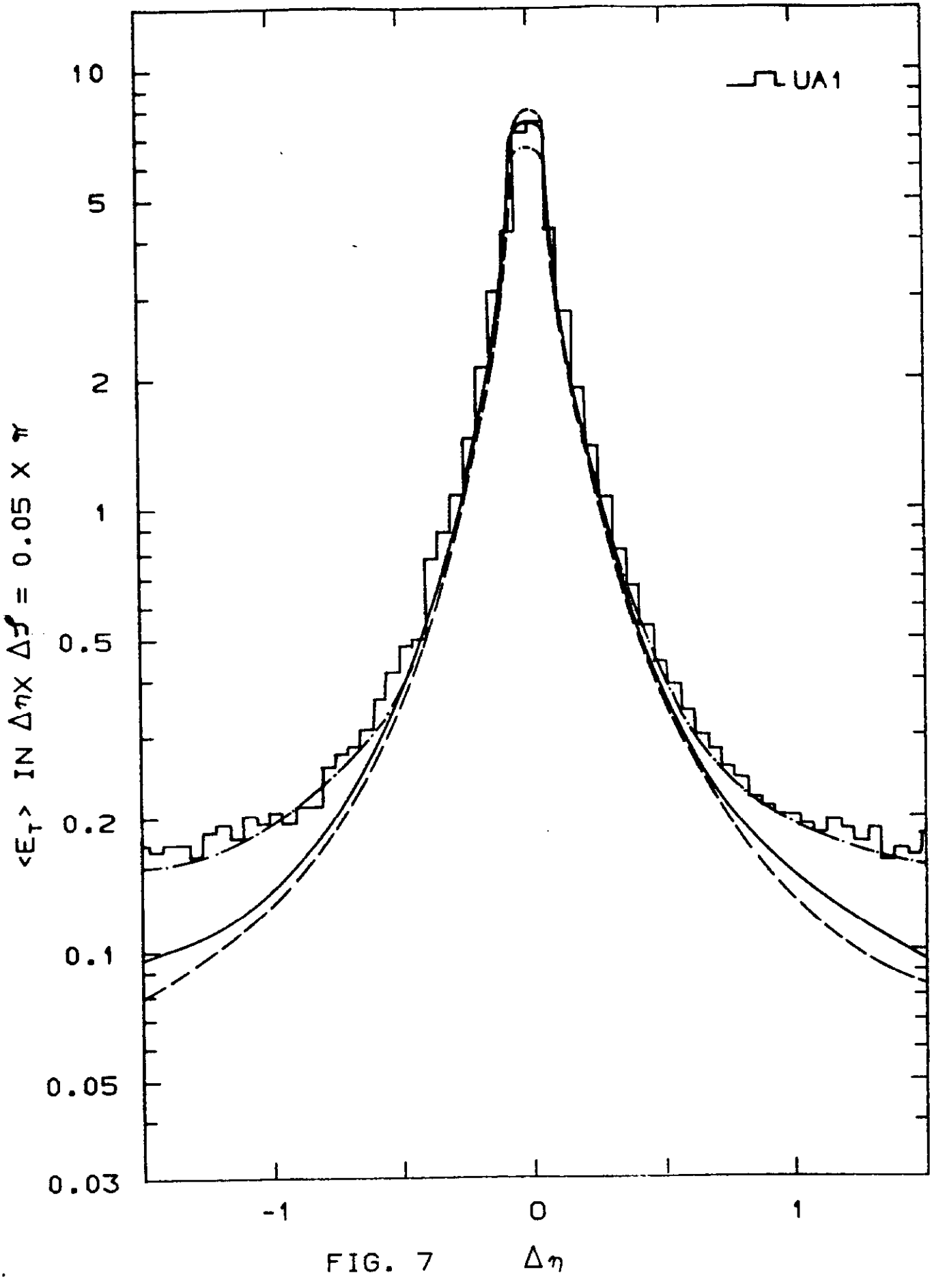
UA1
10
5
2
1
0.5
0.2
0.1
0.05
0.03
-1
0
1
$\Delta\eta$
$\langle E_T \rangle$ IN $\Delta\eta$X $\Delta\phi$ = 0.05 X π

FIG. 7

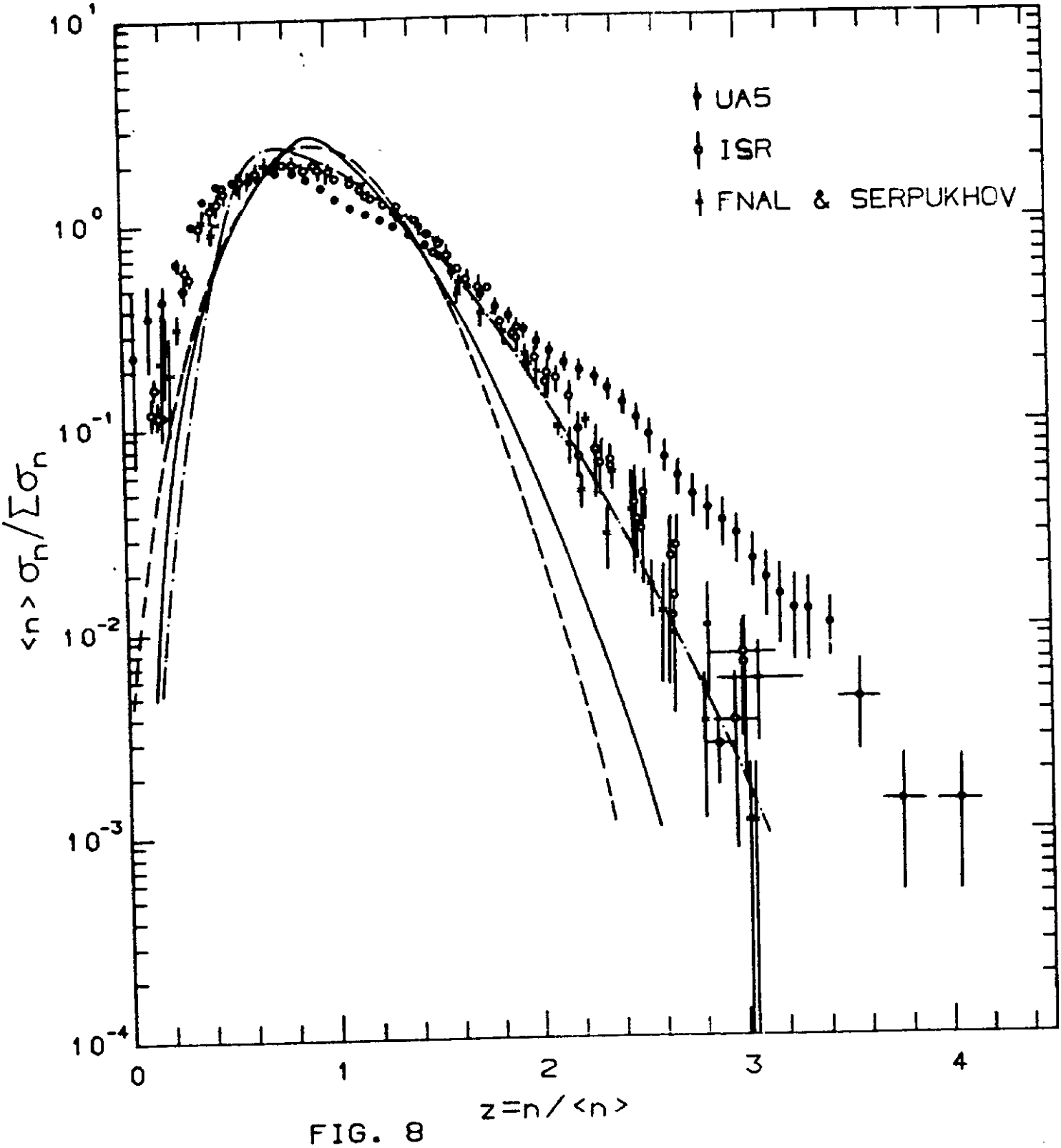
UA5
ISR
FNAL & SERPUKHOV
10^1
10^0
10^{-1}
10^{-2}
10^{-3}
10^{-4}
$\langle n \rangle \sigma_n / \Sigma \sigma_n$
0
1
2
3
4
$z = n / \langle n \rangle$

FIG. 8

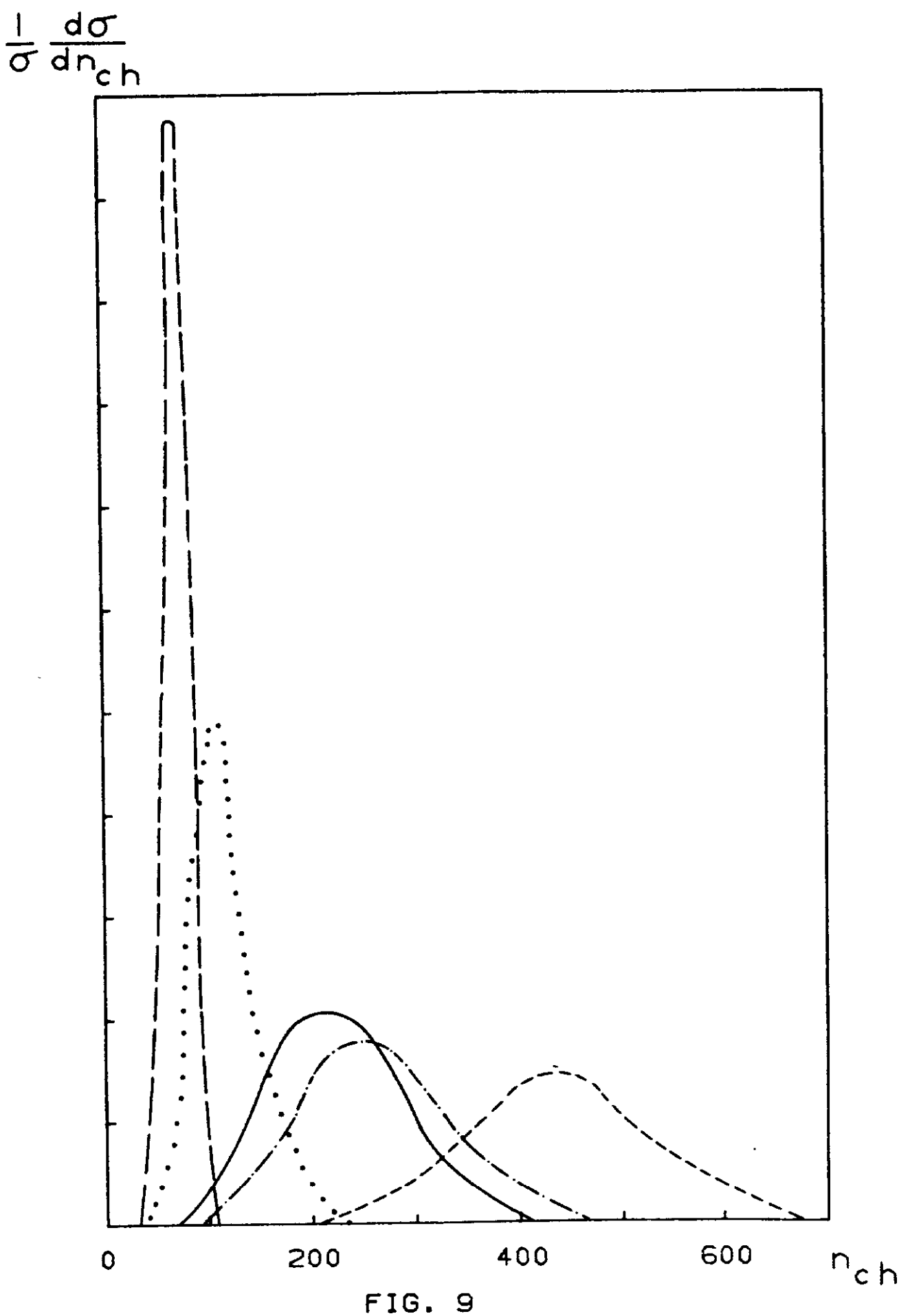

FIG. 9